Blood Glucose Level Prediction Using Subcutaneous Sensors for in Vivo Study: Compensation for Measurement Method Slow Dynamics Using Kalman Filter Approach

Martha Halvorsen, Karim Davari Benam*, Hasti Khoshamadi*, Anders Lyngvi Fougner

***Abstract*— The continuous glucose monitoring (CGM) system is the most common system used by people with type 1 diabetes to monitor blood glucose levels. However, it measures glucose in interstitial fluid in subcutaneous tissue rather than directly in plasma. Measuring blood glucose level in this method has slow dynamics and introduce a time lag in capturing the blood glucose level. This can reduce the quality of blood glucose regulation and result in hypo- or hyperglycemia. In this paper, a linear Kalman filter is developed to predict blood glucose concentration using CGM data to compensate for that slow dynamics. To this end, an observable input-less model describing the glucose diffusion from plasma to interstitial fluid is utilized. Notably, this model is physiology-based, and its parameters can be obtained from the literature. The designed structure is evaluated on data from two animal experiments conducted on anesthetized pigs. The data sets include CGM measurements every 1.2 seconds and sporadic blood sample analysis during experiments. Results show that the designed approach sufficiently can compensate for the slow dynamics of CGM measurements when compared to blood glucose samples, and the performance is measured using statistical accuracy scores. This compensation can improve the decision-making of control algorithms for glucose regulation during rapid changes in glucose concentration, e.g., during meals and exercise.**

I. INTRODUCTION

Diabetes mellitus is a metabolic disorder or disease that affects approximately 537 million adults worldwide as of 2021 [1]. It is characterized by chronic hyperglycemia in response to ingestion of carbohydrates, fat, and protein, resulting from defects of insulin secretion, insulin action, or both [2]. In a healthy individual, glucose regulation is performed by two hormones, insulin, and glucagon, produced in the pancreas. Insulin secretion makes the glucose concentration in the blood decrease, while glucagon secretion increases the blood glucose (BG) concentration [2]. In type 1 diabetes mellitus (T1DM), the pancreas does not produce insulin due to the destruction of beta cells, which produce insulin in the pancreas [3]. Hence the insulin must be administered by an external source [2]. As a result, people with type 1 diabetes require daily insulin treatment, regular BG monitoring, and a healthy lifestyle to manage their condition effectively [4].

In 1999 diabetes technology made huge progress when the continuous glucose monitoring (CGM) system was approved by the Food and Drug Administration (FDA) and became commercially available [5]. The CGM sensor is placed in the subcutaneous tissue and measures glucose levels in the interstitial fluid in real-time [2]. The minimally invasive structure of the sensor system allows for continuous glucose measurements, eliminating the need for self-monitoring systems, e.g., finger prick [5]. In addition, continuous glucose measurements provide BG trends and fluctuations.

Despite the sensor's revolutionary qualities, it is not without problems. One of its disadvantages is that the sensor measures ISF glucose level rather than plasma glucose level. Due to plasma-to-ISF glucose dynamics, the CGM measurements are delayed compared to measurements taken directly from the blood during rapid changes in BG [6]. The plasma-to-ISF glucose dynamics refers to glucose diffusion across capillaries and through the interstitial space where the sensor is located [6]. Hence, during both BG rising and falling, the time of the diffusion process will result in the ISF glucose lagging behind the BG. The slow dynamics between these two compartments, together with sensor processing time, causes about, on average, a $4-10\,\mathrm{min}$ lag between the BG and the sensor readings [2].

Control algorithms, along with CGM sensors and infusion pumps, are employed in commercially available control devices (artificial pancreas) to regulate BG levels in patients with T1DM. Based on the CGM measurements, the control algorithm will automatically infuse the optimal amount of insulin, and glucagon, in a timely manner. Notably, the absorption and effect of hormones are not instantaneous. Hence, using CGM measurements can lead to a late response to BG level fluctuations which in turn cause severe low or high BG levels. Therefore, predicting the BG levels can help artificial pancreas systems to improve glycemic control.

There are several ways proposed in the literature for predicting or estimating the blood glucose level using CGM measurements. The deconvolution approach is employed to reconstruct the plasma glucose from ISF glucose measurements in [7]. However, it is concluded that perfect linearity and time invariance of the system is required for this method. In addition, various works have addressed the problem through the use of Kalman filtering. In [8], a physiological model is considered for the glucose diffusion from plasma to

This research is funded by the Research Council of Norway (project no. 248872), and the Centre for Digital Life Norway. Inreda Diabetic (Goor, the Netherlands) provided transmitters, materials and hormones infusion systems (AP3) for animal experiments at no cost.

M. Halvorsen, K.D. Benam, H. Khoshamadi, and A.L. Fougner are with Department of Engineering Cybernetics, Faculty of Information Technology and Electrical Engineering, Norwegian University of Science and Technology (NTNU), O. S. Bragstads Plass 2D, 7034 Trondheim, Norway. martha.halvorsen@gmail.com, {karim.d.benam, hasti.khoshamadi, anders.fougner}@ntnu.no

*These authors contributed equally to this work

ISF glucose dynamic; nevertheless, it is assumed that plasma glucose changes randomly in a step or rate fashion. In [9], the Kalman filter estimates plasma glucose and sensor gain from CGM and fingerstick measurements. In this approach, both plasma glucose level and sensor gain are modeled as ramp disturbances; however, the time lag between plasma and ISF glucose is neglected. A smoothing Kalman filter is used in [10] in an offline manner to interpolate BG measurements when blood samples are taken irregularly utilizing the CGM and fingerstick measurements. The smoothing Kalman filter is based on the central-remote rate model proposed for plasma glucose dynamics. Moreover, the plasma-to-ISF dynamic is also combined in the model. This Kalman smoother was not applied in the current study because it is non-causal.

In this paper, the Kalman filter, together with the input-less model introduced in [10] is utilized to estimate the BG level and compensate for the slow plasma-to-ISF dynamics. The proposed structure is tested on data from animal experiments, and the performance is analyzed using standard statistical methods. To the author's knowledge, the application of the proposed method to the real-life scenarios of anesthetized animal experiments, having the CGM system with a high sampling rate (every 1.2 seconds), frequent measurements of the blood gas analyzer (BGA) to evaluate the performance of the estimator, and together with the use of the intraperitoneal route for insulin and glucagon infusions are novel in the subject.

The paper is structured as follows. The data used in this paper is described in Section II. A brief description of the standard linear Kalman filter is given in Section III, a plasma-to-ISF glucose dynamics model is introduced in Section IV and evaluation tools and metrics for measuring filter performance are given in V. The results are presented in VI, and are discussed in VII, before a conclusion is provided in Section VIII.

II. Data

The data used for the simulations in this paper is collected through two animal experiments performed in the animal faculty of the University of Norwegian science and technology. These experiments were conducted on two anesthetized pigs whose endogenous insulin and glucagon secretions were suppressed using Octreotide (Sandostatin) with a rate of 5 µg/kg/h. In addition, intravenous glucose infusion (with a concentration of 200mg/ml) was used to simulate different meals in the anesthetized animal experiments. In order to control the BG level, intraperitoneal insulin and glucagon administrations were used.

The CGM sensors used in these experiments were the Medtronic Enlite sensor (Northridge, Canada). These sensors were paired with custom transmitters from Inreda Diabetic (Goor, the Netherlands), providing measurements with a sampling rate of $1.2\,\mathrm{s}$. In order to measure the BG level directly, blood samples were taken sporadically, varying between every $5\,\mathrm{min}$-$1\,\mathrm{hour}$, and analyzed by ABL800 FLEX analyzer (Copenhagen, Denmark), which is a BGA system.

Data set 1 is the collected data from animal experiment 1 and consists of three meals, where the weight of the pig was $36\,\mathrm{kg}$, while data set 2 the collected data from animal experiment 2 and consists of four meals, where the weight of the pig was also $36\,\mathrm{kg}$. The CGM measurements are plotted together with the BGA measurements for data set 1 and for data set 2 in (1).

III. Kalman filter

The Kalman filter is a recursive filter that uses a time series of measurements in order to estimate the internal states of a linear dynamical system. Given an output signal y_k, any time-invariant discrete system can be assumed to be modelled as follows:

$$x_{k+1} = Fx_k + Bu_k + w_k \tag{1}$$
$$y_k = Hx_k + v_k \tag{2}$$

where $x_k \in \mathbb{R}^n$, $u_k \in \mathbb{R}^p$, and $y_k \in \mathbb{R}^m$ is the system state, system input and the system output vectors at time iteration k, respectively. Moreover, F is the state transition matrix, B is the input transition matrix, and H is the measurement matrix. Assume that the system matrices all have appropriate dimensions. The process and measurement noises are denoted by w_k and v_k which satisfy the following conditions:

$$\begin{aligned} w_k &\sim (0, Q) \\ v_k &\sim (0, R) \\ E[w_k w_j^T] &= Q\delta_{k-j} \\ E[v_k v_j^T] &= R\delta_{k-j} \\ E[v_k w_j^T] &= 0. \end{aligned} \tag{3}$$

where Q and R are covariance matrices of process and measurement noises respectively. In addition, δ_{k-j} is the Kronecker delta function which gives $\delta_{k-j} = 1$ if $k = j$, and $\delta_{k-j} = 0$ if $k \neq j$ [11].

The Kalman filter computes an estimate of the internal states, $\hat{x}$, as well the estimation error covariance matrix, P_k, for each time iteration k. P_k can be considered as a tool to evaluate of the quality the current estimate $\hat{x}_k$ quantitatively [12].

The estimation process is performed in two steps, a *prediction step*, and a *correction step*. In the prediction step the filter uses the model from (1) to predict the states one iteration ahead of time. The resulting estimate is known as the *a priori estimate*, and will be denoted as $\bar{x}_{k+1}$ and $\bar{P}_{k+1}$. In the following correction step the *a priori estimate* is used in combination with the measurement y_k to update and improve the *a posteriori estimate*, which is denoted $\hat{x}_{k+1}$ and $\hat{P}_{k+1}$.

Hence the Kalman filter equations are given by the followings [11]:

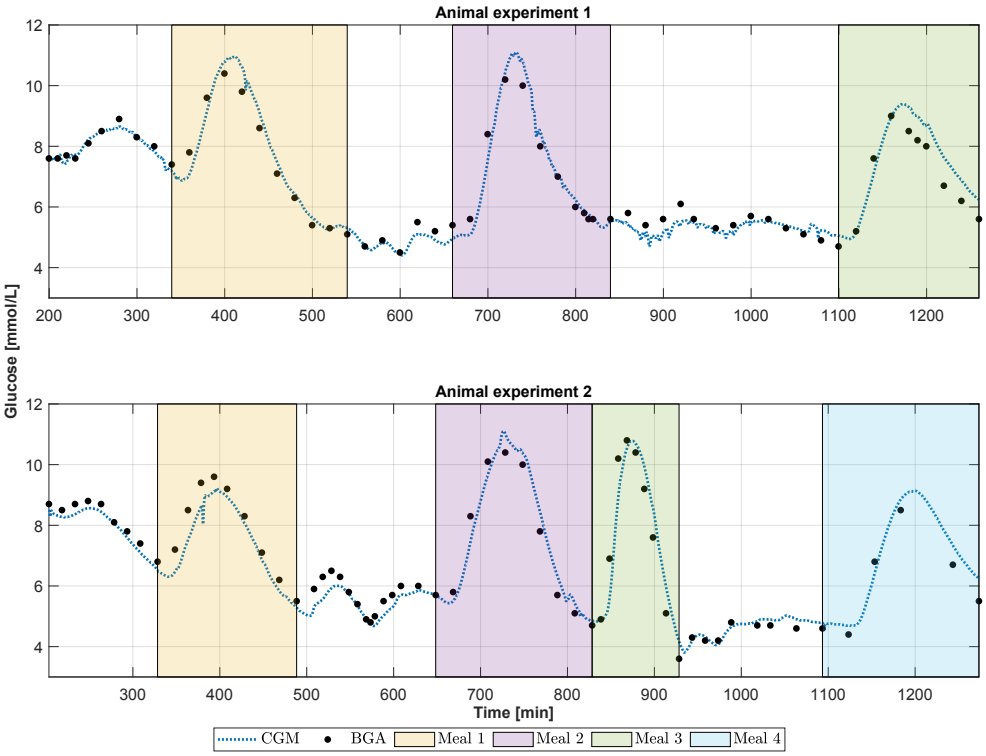

Fig. 1: Continuous glucose monitoring (CGM) and blood gas analyzer (BGA) measurements sectioned by color into specific meal times. The top row describes the data set from animal experiment 1, with three observed meal times, while the bottom row describes the data set from animal experiment 2, with four observed meal times.

Prediction:

$$\begin{aligned} \bar{x}_{k+1} &= F\hat{x}_k + Bu_k \\ \bar{P}_{k+1} &= FP_kF^T + Q \end{aligned} \tag{4}$$

Correction:

$$\begin{aligned} K_k &= \bar{P}_{k+1}H^T(H\bar{P}_{k+1}H^T + R)^{-1} \\ \hat{x}_{k+1} &= \bar{x}_{k+1} + K_k(y_k - H\bar{x}_{k+1}) \\ P_{k+1} &= (I - K_kH)\bar{P}_{k+1}. \end{aligned}$$

where K_k is the Kalman gain matrix at time iteration k. The dynamical system given by (1) and (2) must be fully observable for the Kalman filter to obtain optimal estimates of all internal states. When a system is fully observable, the observability given by (5) is full rank.

$$O = \begin{bmatrix} H \\ HF \\ \vdots \\ HF^{n-1} \end{bmatrix} \tag{5}$$

IV. Mathematical Model

Using a Kalman filter requires a mathematical, dynamic model describing the system. Models describing the glucose dynamics are not limited in the literature, and they range from minimal [13] to quite complex [14]. Models like these describe the glucose dynamics where insulin and meals are inputs of the system. Using such models requires precise information about inputs and parameters, which is not always available or bears the quality needed. In this paper, the introduced model in [10] which combines the ISF glucose dynamics with a plasma glucose dynamical model is used. The combined model makes it possible to have plasma glucose as a state of the system, which is observable with CGM measurement. Notably, insulin and meals are treated as unknown system disturbances in this model.

A. Plasma-ISF Glucose Dynamics

The Steil-Rebrin model is a model describing the ISF glucose dynamics, using a two compartmental structure as follows [15], [16] :

$$\frac{dG_{isf}}{dt}(t) = -(k_{02} + k_{12})G_{isf}(t) + k_{21}\frac{V_1}{V_2}G_p(t). \tag{6}$$

where k_{02} is the glucose uptake rate of subcutaneous tissue from ISF, k_{12} and k_{21} are diffusion rates between plasma and ISF compartments, V_1 and V_2 are volumes of the plasma and ISF glucose compartments, respectively [11]. G_{isf} describes the glucose concentration in ISF, and G_p describes the glucose concentration in plasma. The relationship between the plasma glucose concentration and the ISF glucose concentration can be further simplified:

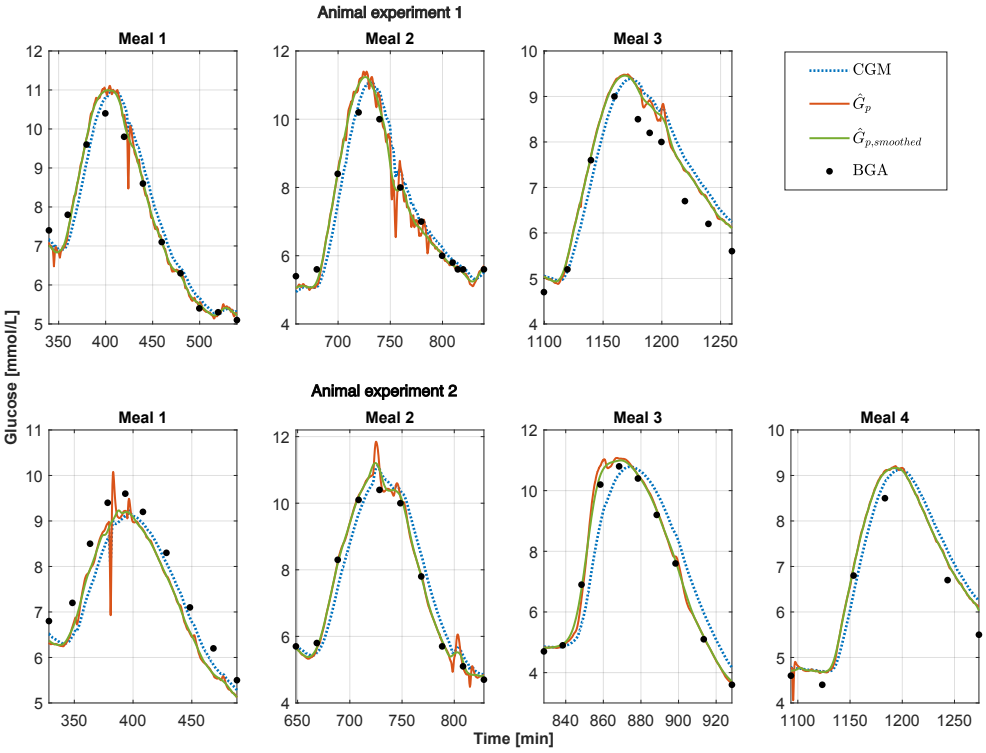

Fig. 2: Kalman filter estimate, $\hat{G}_p$, plotted together with the moving average smoothed Kalman filter estimate, $\hat{G}_{p,smoothed}$, where Continuous glucose monitoring (CGM) measurements and blood gas analyzer (BGA) measurements are shown for comparison.

$$\frac{dG_{isf}}{dt}(t) = -\frac{1}{T_{isf}}G_{isf}(t) + \frac{g}{T_{isf}}G_p(t), \tag{7}$$

where T_{isf} is the diffusion time constant, and g is a steady-state gain. These parameters are defined as follows:

$$T_{isf} \triangleq \frac{1}{k_{02}+k_{12}} \tag{8}$$

$$g \triangleq \left(k_{21}\frac{V_1}{V_2}\right)T_{isf} \tag{9}$$

Notably, in the steady state, $g = G_{isf}/G_p$. Physiologically, for a given change in plasma glucose concentration, the same long-term change in the ISF glucose concentration is expected, and thus $g = 1$ [7], [11].

B. Central-Remote Rate Model

The plasma glucose model is divided into a central compartment, C_c, and a remote compartment, C_r. Insulin or meals going into the system will first affect the central compartment before it diffuses over to the remote compartment by a first-order delay [10], where it finally causes changes in the plasma glucose concentration, G_p. The state-space equations are as followings:

$$\begin{aligned}
\frac{dG_p}{dt}(t) &= C_r(t) \\
\frac{dC_c}{dt}(t) &= -\frac{1}{T_d}C_c(t) \\
\frac{dC_r}{dt}(t) &= \frac{1}{T_d}(C_c(t) - C_r(t)),
\end{aligned} \tag{10}$$

where T_d is a time constant, describing the diffusion rate between the central and remote compartments [10].

C. Combined Model

The models from (IV-A) and (IV-B) are combined to create a fully observable system in which the plasma glucose concentration is part of the state vector. At the same time, it also provides an insight into plasma glucose dynamics. The state-space form of this combined model is given by:

$$\begin{bmatrix} \dot{G}_{p,k} \\ \dot{C}_{c,k} \\ \dot{C}_{r,k} \\ \dot{G}_{isf,k} \end{bmatrix} = \begin{bmatrix} 0 & 0 & 1 & 0 \\ 0 & -\frac{1}{T_d} & 0 & 0 \\ 0 & \frac{1}{T_d} & -\frac{1}{T_d} & 0 \\ \frac{1}{T_{isf}} & 0 & 0 & -\frac{1}{Tisf} \end{bmatrix} \begin{bmatrix} G_{p,k} \\ C_{c,k} \\ C_{r,k} \\ G_{isf,k} \end{bmatrix} + w_k$$

$$y_k = \begin{bmatrix} 0 & 0 & 0 & 1 \end{bmatrix} \begin{bmatrix} G_{p,k} \\ C_{c,k} \\ C_{r,k} \\ G_{isf,k} \end{bmatrix} + v_k, \tag{11}$$

TABLE I: Mean absolute error (MAE) and mean absolute percentage error (MAPE) scores for the continuous glucose monitoring (CGM) measurements, the Kalman filter blood glucose estimate, $\hat{G}_p$ and for the moving average smoothed Kalman filter estimate, $\hat{G}_{p,smoothed}$, where blood gas analyzer (BGA) is considered as the reference blood glucose level.

		MAE [mmol/L]			MAPE [%]		
		CGM	$\hat{G}_p$	$\hat{G}_{p,smoothed}$	CGM	$\hat{G}_p$	$\hat{G}_{p,smoothed}$
Data set 1	Meal 1	0.38	0.24	0.21	4.82	2.99	2.61
	Meal 2	0.34	0.31	0.20	4.68	4.17	2.69
	Meal 3	0.55	0.47	0.45	8.02	6.90	6.60
	All	0.32	0.30	0.25	4.68	4.36	3.72
Data set 2	Meal 1	0.46	0.48	0.50	5.78	6.47	6.55
	Meal 2	0.43	0.16	0.17	5.86	2.03	2.22
	Meal 3	0.65	0.21	0.13	9.53	2.71	1.86
	Meal 4	0.44	0.37	0.34	7.30	6.12	5.55
	All	0.40	0.28	0.27	5.84	4.11	3.98

where the dot notation is equivalent to the time-derivative notation, i.e $\dot{x} = \frac{dx(t)}{dt}$. Notably, by assuming A as the continuous state transition matrix of the combined systems of eq. (10) and eq. (7), the combined system is discretized by setting the discrete state transition matrix equal to $e^{A\Delta t}$, where the time step Δt is set to $\frac{1.2}{60}$ min (in which $1.2\,\mathrm{sec}$ is the CGM sampling time).

V. Metrics

To evaluate the performance of the filter more in detail, the mean absolute error (MAE) and mean absolute percentage error (MAPE) are used, which are defined as below:

$$\mathrm{MAE} = \frac{1}{n}\sum_{i=1}^{n}|e_i|, \tag{12}$$

$$\mathrm{MAPE} = \frac{1}{n}\sum_{i=1}^{n}\frac{|e_i|}{y_i}100\%, \tag{13}$$

with

$$e_i = y_i - \hat{y}_i, \tag{14}$$

where y_i and $\hat{y}_i$ are the real value and the estimate of that, respectively, and n is the total number of samples. The more accurate the method, the smaller the resulting values for MAE and MAPE.

In the calculation of MAE and MAPE, the CGM measurements, the Kalman filter estimate ($\hat{G}_p$), and the smoothed estimates ($\hat{G}_{p,smoothed}$) are compared with the BGA measurement as the reference value. As the BGA samples were taken sporadically while CGM sensor readings and the estimates via Kalman filter are available every $1.2\,\mathrm{sec}$, the error is calculated based on BGA samples and their closest corresponding samples in CGM readings or Kalman filter estimates.

VI. Results

In order to predict the BG level using the CGM measurements, a Kalman filter is utilized. This filter is designed based on the model given in (11). In this model, T_d is set to $10\,\mathrm{min}$ as in [10], and T_{isf} is set to $7\,\mathrm{min}$, as the middle point of what has been reported in the literature ($4-10\,\mathrm{min}$) [2]. The process noise covariance Q and the measurement noise covariance R are given in as followings, respectively.

$$Q = \begin{bmatrix} 0.01 & 0 & 0 & 0 \\ 0 & 0.01 & 0 & 0 \\ 0 & 0 & 0.01 & 0 \\ 0 & 0 & 0 & 0.01 \end{bmatrix}, R = 2 \tag{15}$$

The Kalman filter estimates, as well as CGM measurements and BGA samples for each of the two animal experiments, are shown in fig. 2. This figure describes specifically the meals throughout the experiments, which are recognized by rise and fall in the blood glucose concentration. As is shown in fig. 2, the Kalman filter successfully reconstructed the BG level using the CGM measurements and compensated for what can be interpreted as the time lag due to the glucose diffusion process between plasma and interstitial compartments. The Kalman filter is observed to be oversensitive to small changes in the CGM measurements, hence a moving average smoother is employed to smooth the estimates. Using a moving average function in Matlab with a span of 1000 samples does not make a significant delay in the estimates, but it results in smoothed estimates. The only drawback is the requirement of having enough CGM samples to start the smoother, which is equal to having $20\,\mathrm{min}$ of CGM readings.

In table I, the evaluation scores are calculated for every meal registered in each data set, as well as for the whole time window, with the exception of the calibration interval, from about $0-200\,\mathrm{min}$. As demonstrated in this table, there is a clear trend where the Kalman filter outperforms the CGM system due to the prediction, and the moving average filtering improves the performance of the Kalman filter. Meal 1 in data set 2 is an exception to this trend, showing the best score for MAE and MAPE in the CGM measurements. As shown in Meal 1, data set 2, in fig. 2, approximately no time lag exists between CGM and BGA measurements when glucose is decreasing, implying that the poor performance of the Kalman filter in this meal is more related to the sensor itself rather than the Kalman filter. The importance

of smoothing can be observed in meal 2 of data set 1, where the CGM and the Kalman filter performances do not differ to a high degree, while the smoothed Kalman filter estimate has a significantly lower score for both MAE and MAPE, see table I, and follows the slope of the BGA precisely, see fig. 2. Predictions achieved by the Kalman filter and the smoothed Kalman filter bear more resemblance to the BGA measurements compared to the CGM readings, and for most of the meals the estimates can be seen eliminating what can be interpreted as the slower dynamic of CGM. This is especially evident in Meal 1, Meal 2 and on glucose increase in Meal 3, for data set 1, and Meal 2, Meal 3, and on glucose increase in Meal 4, in data set 2, see fig. 2.

VII. DISCUSSION

For the sake of simplicity, a linear model was used in this study. Future research should examine the impact of model choice on the outcomes and evaluate whether a more sophisticated or even simpler model might enhance the predictions. The parameters of the model are adjusted according to the literature. Hence, given any CGM measurements, the proposed method with the same parameters should be able to predict the BG level without system identification. However, performance degradation might be expected if the CGM sampling rate decreases. In addition, a trial-and-error approach is used to tune the covariance matrices to achieve satisfactory results while a methodical approach to adjust the KF can improve the performance. Moreover, only two data sets have been used in the simulations for evaluation, and in order to achieve more reliable results, the method should be tested on more data sets that are saved for future studies. The proposed method can be used in closed-loop systems and/or state estimators (for example [17]) to decrease the delays in artificial pancreas systems. However, the effectiveness of the suggested method in closed-loop systems may be evaluated by using the control-variability grid analysis (CVGA) method.

VIII. CONCLUSIONS

The glucose diffusion process from plasma to interstitial fluid causes a time lag between BG levels and CGM measurements as the CGM sensor measures glucose in the subcutaneous tissue. The Kalman filter with an input-less model of the glucose dynamics has been used to estimate the BG level based on the CGM measurement. In addition, the Kalman filter estimates were smoothed in order to reduce the Kalman filter sensitivity to the disturbances of CGM readings. Considering the BGA values as the reference, the performance of the CGM sensor, Kalman filter, and moving average smoothed Kalman filter were assessed. Results showed that estimates obtained from both the Kalman filter and moving average smoothed Kalman filter resembled the BGA measurements to a higher degree, than the CGM measurements.

IX. ACKNOWLEDGMENTS

The animal experiments were carried out at the Comparative medicine core facility in the Norwegian University of Science and Technology (NTNU). The study was partly funded by The Norwegian Research Council (with project no. 248872) through the Center for Digital Life Norway. The transmitters and the hormones infusion system are provided by Inreda Diabetic company (Goor, the Netherlands) for this study at no cost. The authors would like to thank Marte Kierulf Åm, Oddveig Lyng, and Patrick Christian Bösch for their contribution to the data collection.

REFERENCES

[1] IDF Diabetes Atlas, "Diabetes around the world in 2021," https://diabetesatlas.org/ (accessed: 22.03.2022), 2021.

[2] A. Cinar and K. Turksoy, *Advances in Artificial Pancreas Systems, Adaptive and Multivariable Predictive Control*. Gewerbestrasse 11, 6330 Cham, Switzerland: Springer International Publishing AG, 2018.

[3] Centers for Diseases Control and Preventing, "What is type 1 diabetes?" https://www.cdc.gov/diabetes/basics/what-is-type-1-diabetes.html (accessed: 22.03.2022), 2022.

[4] International Diabetes Fedartion, "Type 1 diabetes," https://idf.org/aboutdiabetes/type-1-diabetes.html (accessed: 22.03.2022), 2020.

[5] G. Cappon, M. Vettoretti, G. Sparacino, and A. Facchinetti, "Continuous glucose monitoring sensors for diabetes management: A review of technologies and applications," *Diabetes and Metabolism Journal*, vol. 43, no. 4, pp. 383–397, 2019.

[6] G. Schmelzeisen-Redeker, M. Schoemaker, H. Kirchsteiger, G. Freckmann, L. Heinemann, and L. del Re, "Time delay of cgm sensors: Relevance, causes, and countermeasures," *Journal of Diabetes Science and Technology*, vol. 9, no. 5, pp. 1006–1015, 2015.

[7] C. C. Andrea Facchinetti, Giovanni Sparacino, "Reconstruction of glucose in plasma from interstitial fluid continuous glucose monitoring data: Role of sensor calibration," *IEEE Transactions on Biomedical Engineering*, vol. 1, no. 3, pp. 671–623, 2007.

[8] B. Bequette, "Optimal estimation applications to continuous glucose monitoring," in *Proceedings of the 2004 American Control Conference*, vol. 1, 2004, pp. 958–962 vol.1.

[9] M. Kuure-Kinsey, C. C. Palerm, and B. W. Bequette, "A dual-rate kalman filter for continuous glucose monitoring," in *2006 International Conference of the IEEE Engineering in Medicine and Biology Society*, 2006, pp. 63–66.

[10] O. M. Staal, S. Salid, A. Fougner, and O. Stavdahl, "Kalman smoothing for objective and automatic preprocessing of glucose data," *IEEE Journal of Biomedical and Health Informatics*, vol. 23, no. 1, pp. 218–226, 2019.

[11] D. Simon, *Optimal Estimation*. John Wiley & Sons, Inc., Hoboken, 2006.

[12] F. Auger, M. Hilairet, J. M. Guerrero, E. Monmasson, T. Orlowska-Kowalska, and S. Katsura, "Industrial applications of the kalman filter: A review," *IEEE Transactions on Industrial Electronics*, vol. 60, no. 12, pp. 5458–5471, 2013.

[13] C. Claudio, M. Chiara, Dalla, T. Gianna, B. Rita, V. Adrian, and R. Rizza, "The oral minimal model method," *Diabetes*, vol. 63, no. 4, p. 1203–1213, 2014.

[14] C. D. Man, F. Micheletto, D. Lv, M. Breton, B. Kovatchev, and C. Cobelli, "The uva/padova type 1 diabetes simulator: New features," *Journal of Diabetes Science and Technology*, vol. 8, no. 1, pp. 26–34, 2014.

[15] T. Koutny, "Blood glucose level reconstruction as a function of transcapillary glucose transport," *Computers in Biology and Medicine*, vol. 53, pp. 171–178, 2014.

[16] K. Rebrin, G. M. Steil, W. P. van Antwerp, and J. J. Mastrototaro, "Subcutaneous glucose predicts plasma glucose independent of insulin: implications for continuous monitoring," *American Journal of Physiology-Endocrinology and Metabolism*, vol. 277, no. 3, pp. E561–E571, 1999.

[17] K. D. Benam, H. Khoshamadi, L. Lema-Pérez, S. Gros, and A. L. Fougner, "A nonlinear state observer for the bi-hormonal intraperitoneal artificial pancreas," in *2022 44th Annual International Conference of the IEEE Engineering in Medicine & Biology Society (EMBC)*. IEEE, 2022, pp. 171–176.